Ruthenium(III)–aminopolycarboxylato complexes active for the reduction of the N–N bond of hydrazine and phenylhydrazine in aqueous acidic media

Raju Prakash and Gadde Ramachandraiah *

Discipline of Reactive Polymers, Central Salt and Marine Chemicals Research Institute, Gijubhai Badheka Marg, Bhavnagar 364 002, India

Interactions of hydrazines $N_2H_4X^+$ (X = H or Ph) with tri-, tetra- and penta-chelated ruthenium(III)–aminopolycarboxylic acid complexes giving the respective monomeric hydrazinium (Ru^{III}–$N_2H_4X^+$) adducts have been investigated by potentiometry, spectrophotometry and voltammetry in aqueous acidic solution at 25 °C. The deprotonation and metal hydrolysis constants of the complexes and their $N_2H_4X^+$ adducts in 0.1 M Na_2SO_4 solution were determined. At pH 2.8, the complexes exhibited a quasi-reversible one-electron reduction wave of $Ru^{III} \longrightarrow Ru^{II}$ in sampled dc in the potential range between −0.16 and −0.37 V *vs.* SCE, while their hydrazinium adducts obtained *in situ* by adding an excess of $N_2H_4X^+$ showed an additional two-electron reduction wave assigned to Ru^{III}–$N_2H_4X^+ \longrightarrow Ru^I$–$N_2H_4X^+$ in the potential range of −0.02 to −0.35 V *vs.* SCE. The species Ru^I–$N_2H_4X^+$ on successive decomposition and hydrolysis give one mole of each of NH_3, NH_2X and ruthenium(III) species. Further, the Ru^{III}–$N_2H_4X^+$ complexes have been used as electro-catalysts for the reduction of $N_2H_4X^+$ to NH_3 and NH_2X at a mercury pool cathode in acidic solutions of pH 1.9 and 2.8. The quantity of ammonia produced in all cases is linear with time. The $E_{1/2}$ of Ru^{III}–$N_2H_4X^+ \longrightarrow Ru^I$–$N_2H_4X^+$ and the turnover number are correlated with the sigma basicity (ΣpK_a) of the aminopolycarboxylic acids and the results are discussed in terms of the hydrolytic tendency of the metal, the number of co-ordinating groups and the steric repulsion caused by the increase in size of the aminopolycarboxylic acid.

Introduction

Studies on the reactivity of hydrazine at the potential co-ordination site of an active metal centre in the absence and the presence of reducing agents have immense value, since the reduction of dinitrogen to ammonia catalysed by transition metals present in microorganisms[1–7] or simple metal complexes or clusters has long been proposed to proceed *via* metal bound hydrazine. In the recent past intensive research has been carried out to evolve a simple mechanism for dinitrogen fixation. In this respect, numerous transition metals, cofactors and model compounds containing hydrazine were synthesized and characterized.[8–10] Structural analyses of a few of these complexes have also been made.[8,11] Meanwhile, reduction studies were also performed on hydrazine or its derivatives to ammonia and/or amine in both aqueous and non-aqueous solutions either in the absence or in the presence of external proton and electron sources or reducing agents.[12–14] Although, fairly good turnovers of ammonia have reportedly been obtained in organic solvents, most of these reactions did not meet much success in aqueous solutions. However, Schrauzer *et al.*[15] reported the reduction of hydrazine to ammonia using $K_2[Mo(O)(H_2O)(CN)_4]$ as a catalyst and $NaBH_4$ as reducing agent with a turnover rate of 4.2 in aqueous solutions. Later catalytic conversion of hydrazine into ammonia was obtained by $[Mo_2Fe_6S_8L_9]^{3-}$ or $[Fe_4S_4L_4]^{2-}$ (L = SPh or SCH_2CH_2OH) with a moderate turnover number.[16] In another report,[17] $[WCp*Me_3(\eta^2-NH_2NH_2)][O_3SCF_3]$ prepared from $[WCp*Me_3(O_3SCF_3)]$ and N_2H_4 was shown to undergo reduction by Na–Hg to give NH_3. Recently, the co-ordinatively unsaturated diruthenium complex $[Cp*Ru(\mu-SPr^i)_2RuCp*]$ has been reported to catalyse the reduction of hydrazine more effectively.[18] More sophisticated systems $[MoFe_3S_4Cl_3(Cl_4C_6O_2)(MeCN)]^{2-}$ and $[MoFe_3S_4Cl_3(citr)]^{3-}$ (citr = citrate) were also modelled and used to catalyse

the reduction of N_2H_4 to NH_3 with good turnovers by $CoCp_2$ and 2,6-dimethylpyridine hydrochloride.[13,19] Moreover, the N_2H_4-bridged double cubane $[\{MoFe_3S_4Cl_3(Cl_4C_6O_2)\}_2(\mu-NH_2NH_2)]$ was isolated and its catalytic activity studied.[20] However, the parallel evolution of hydrogen gas which reduces the yield of NH_3 was reported as the major limiting step in almost all the above systems.

Recently, we have reported the electrochemical reduction of hydrazine and its phenyl derivative to NH_3 and/or NH_2X at high turnover rates and high coulombic efficiency[21–24] without the liberation of hydrogen gas using terminally co-ordinated Ru^{III}–edta–$N_2H_4X^+$ complexes as electro-catalysts in aqueous acidic solutions. In continuation, herein we describe the interaction of $N_2H_4X^+$ (X = H or Ph) with tri-, tetra- and penta-chelated aminopolycarboxylates of ruthenium(III), *viz.* $K_2[Ru(imda)Cl_3]\cdot2H_2O$ **1**, $K_2[Ru(himda)Cl_2]\cdot H_2O$ **2**, $K_2[Ru(nta)Cl_2]\cdot H_2O$ **3**, $K[Ru(hedta)Cl]$ **4**, $K[Ru(Hedta)Cl]\cdot2H_2O$ **5**, $K[Ru(Hpdta)Cl]\cdot2H_2O$ **6**, $K[Ru(Hcdta)Cl]\cdot H_2O$ **7** and $K[Ru(H_2dtpa)Cl]$ **8** by potentiometry, spectrophotometry and voltammetry in aqueous solution. The function of the resulting hydrazinium complexes as catalysts for the reduction of hydrazine and its phenyl derivative electrochemically in acidic solution is elucidated. The effects of the sigma basicity (ΣpK_a) of the aminopolycarboxylic acid in complexes **1–8** on the half-wave potential ($E_{1/2}$) of the two-electron reduction wave of Ru^{III}–$N_2H_5^+$ complexes and the turnover number of NH_3 produced in the electrolytic reduction of $N_2H_4X^+$ have been investigated.

Experimental

Ruthenium trichloride ($RuCl_3\cdot xH_2O$) from Arora Matthey India, iminodiacetic acid (H_2imda), *N*-(2-hydroxyethyl)imino-diacetic acid (H_2himda), nitrilotriacetic acid (H_3nta), *N*-carb-

oxymethyl-N'-(2-hydroxyethyl)ethylenediiminodiacetic acid (H$_3$hedta), propylenedinitrilotetraacetic acid (H$_4$pdta), (±)-*trans*-cyclohexane-1,2-diyldinitrilotetraacetic acid (H$_4$cdta), and carboxymethyliminobis(ethylenenitrilo)tetraacetic acid (H$_5$dtpa) from Aldrich Chemical Company Inc. USA were purchased. Ethylenedinitrilotetraacetate disodium salt (Na$_2$H$_2$edta) from Polypharm India, hydrazine sulfate (N$_2$H$_5$HSO$_4$) from BDH Chemicals, India and phenylhydrazine hydrochloride (N$_2$H$_4$PhCl) from Allied Chemicals, USA. The zero grade Ar gas from IOLAR & Co. was used after purification with vanadium sulfate and alkaline pyrogallol solutions. All other reagents used were of AR grade. A mixture of 0.2 M CH$_3$COONa and 18 N H$_2$SO$_4$ solutions at a desired pH between 1 and 5 was used as supporting electrolyte in all voltammetric studies. Stock solutions of N$_2$H$_5$HSO$_4$ (0.1 M) were prepared and standardized with potassium iodate.[21] A freshly prepared solution of 0.1 M N$_2$H$_4$PhCl was used to prepare the experimental solutions.

Preparations

K$_2$[RuCl$_5$(OH$_2$)]. The compound was prepared by the method reported elsewhere,[25] and used as the precursor to synthesize three- to five-co-ordinated ruthenium(III)–aminopolycarboxylic acid complexes **1**–**8** according to the following methods.

K$_2$[Ru(imda)Cl$_3$]·2H$_2$O 1. To a hot solution of 10 mL K$_2$-[RuCl$_5$(OH$_2$)] (0.375 g, 1 mmol) in 1 mM HClO$_4$, H$_2$imda (0.136 g, 1.02 mmol) dissolved in 10 mL of 1 mM HClO$_4$ was added slowly with constant stirring. The resultant mixture was refluxed (two hours) till the reddish brown colour changed to pale yellow. Later, the volume of the solution was reduced (5 mL) *in vacuo* on a Rotovapour. It was then precipitated with cold absolute alcohol, filtered off, washed with 9:1 acetone–water till free of chloride and dried under vacuum. Calc. for C$_4$H$_9$Cl$_3$K$_2$NO$_6$Ru: C, 10.46; H, 1.92; N, 3.07. Found: C, 10.60; H, 2.01; N, 3.09%. IR (KBr): 1635 (COO$^-$ asym); 1365 (COO$^-$ sym); 1210 (CO); 840 (OCO def); 535 cm^{-1} (M–N). UV-vis, λ/nm (ε/M^{-1} cm^{-1}): 240 (2270); 285 (1400) and 365 (445).

K$_2$[Ru(himda)Cl$_2$]·H$_2$O 2. The compound **2** was prepared from K$_2$[RuCl$_5$(OH$_2$)] (0.375 g, 1 mmol) and H$_2$himda (0.180 g, 1.02 mmol) by the procedure described for **1**. Calc. for C$_6$H$_{10}$Cl$_2$K$_2$NO$_6$Ru: C, 16.04; H, 2.32; N, 3.09. Found: 16.29; H, 2.28; N, 3.17%. IR (KBr): 1640 (COO$^-$ asym); 1365 (COO$^-$ sym); 1235 (CO); 825 (OCO def); 535 cm^{-1} (M–N). UV-vis, λ/nm (ε/M^{-1} cm^{-1}): 245 (2595); 285 (2360) and 360 (640).

K$_2$[Ru(nta)Cl$_2$]·H$_2$O 3. This compound was prepared from K$_2$[RuCl$_5$(OH$_2$)] (0.375 g, 1 mmol) and H$_3$nta (0.195 g, 1.02 mmol) in the same manner as described above for **1**. Calc. for C$_6$H$_8$Cl$_2$K$_2$NO$_7$Ru: C, 15.85; H, 1.68; N, 3.13. Found: C, 15.79; H, 1.76; N, 3.07%. IR (KBr): 1635 (COO$^-$ asym); 1358 (COO$^-$ sym); 1230 (CO); 850 (OCO def); 525 cm^{-1} (M–N). UV-vis, λ/nm (ε/M^{-1} cm^{-1}): 285 (2420) and 360 (735).

K[Ru(H$_m$L)Cl]·xH$_2$O {m = 0, x = 0 for L = hedta 4; m = 1, x = 2 for edta 5; m = 1, x = 2 for pdta 6}. These compounds were prepared from K$_2$[RuCl$_5$(OH$_2$)] and the respective aminopolycarboxylic acid according to the procedures reported earlier[26–28] and subsequently characterized by physico-chemical methods.

K[Ru(Hcdta)Cl]·H$_2$O 7. This complex was obtained by treating K$_2$[RuCl$_5$(OH$_2$)] (0.375 g, 1.0 mmol) in 10 mL 1 mM HClO$_4$ with Na$_2$H$_2$cdta (0.400 g, 1.02 mmol) in 20 mL 1 mM HClO$_4$ under a nitrogen atmosphere, initially for 30 min with stirring at room temperature followed by refluxing for about two hours. The greenish yellow solution was evaporated to small volume.

The complex was precipitated with cold absolute ethanol, washed with 9:1 acetone–water solution until free from chloride and dried under vacuum. Calc. for C$_{14}$H$_{21}$ClKN$_2$O$_9$Ru: C, 31.32; H, 4.19; N, 5.14. Found: C, 31.20; H, 4.30; N, 5.20%. IR (KBr): 3450 (OH); 1750 (COOH); 1655 (COO$^-$ asym); 1375 (COO$^-$ sym); 1220 (CO); 885, 685 (OCO def); 520 cm^{-1} (M–N). UV-vis, λ/nm (ε/M^{-1} cm^{-1}): 240 (2430); 285 (1640) and 370 (700).

K[Ru(H$_2$dtpa)Cl] 8. This complex was isolated from K$_2$-[RuCl$_5$(OH$_2$)] and H$_5$dtpa (0.403 g, 1.02 mmol) in 20 mL of HClO$_4$ by the procedure described in the case of **7**. Calc. for C$_{16}$H$_{20}$ClKN$_3$O$_{12}$Ru: C, 29.82; H, 3.49; N, 7.34. Found: C, 29.7; H, 3.56; N, 7.43%. IR (KBr): 3560 (OH); 1750 (COOH); 1655 (COO$^-$ asym); 1375 (COO$^-$ sym); 1280 (CO); 885, 685 (OCO def); 525 cm^{-1} (M–N). UV-vis, λ/nm (ε/M^{-1} cm^{-1}): 235 (2235); 280 (1560) and 370 (375).

Instrumentation

Perkin-Elmer Series II-2400, CHNS/O Analyzer for C, H, N-data; Bio-Rad FT-40 spectrometer coupled to a SP-3200 computer for IR; Shimadzu UV-vis NIR scanning spectrophotometer UV-3101 PC for absorption spectra. An Adair Dutt digital pH meter (±0.01 pH) was used to record the pH of all experimental solutions other than those in potentiometry.

Electrochemical measurements were performed on EG&G Princeton Applied Research (PARC) instruments. A model PAR 174A Polarographic Analyzer and PAR 175 Universal Programmer coupled to a high precision Houston X-Y recorder were used to record sampled dc polarograms and cyclic voltammograms. A three electrode assembly, PAR 303 SMDE/HMDE comprising a dropping (DME, 3.85 mg s^{-1})/hanging (HMDE, 0.021 cm^2) mercury drop working, platinum wire auxiliary and SCE reference electrodes was employed.

The controlled potential coulometry was performed on a EG&G PAR model 173 Potentiostat/Galvanostat coupled to a model 179 digital coulometer provided with a three electrode cell assembly. The cell consisted of a mercury pool (4 cm convex diameter) working electrode in the main compartment along with a platinum mesh as counter electrode separated by a glass frit, SCE reference electrode and a glass disc agitator. An Orion 940 Ion Analyzer equipped with a model 9512 ammonia sensing membrane electrode (sensitive to 10^{-12} M) was used for the estimation of ammonia in the electrolysed solutions.

Analytical methods

All acid–base titrations were conducted in a jacketed glass-walled cell of about 150 mL capacity, connected to a Metrohm Swiss model 682 Auto Titroprocessor coupled with a 665 Dosimat and E-649 magnetic stirrer, through a combined glass-reference electrode. The cell also had inlet and outlet tubes for passing Ar gas through the solution. The electrode system was calibrated in terms of H$^+$ concentration by means of a titration of HCl solution with NaOH[29] in 0.1 M Na$_2$SO$_4$ at 25 ± 0.1 °C. The experimental data ranged over pH values between 1.6 and 11.2.

In a typical experiment, a weighed quantity of a complex **1**–**8**, N$_2$H$_5$HSO$_4$ or N$_2$H$_4$PhCl (1 mM) was dissolved in 50 mL of 0.1 M Na$_2$SO$_4$ and titrated independently against carbonate free (0.1 M) NaOH solution in the region 2 < pH < 10 under Ar at 25 °C. Similar titrations were conducted in the presence of 1 equivalent of N$_2$H$_5$HSO$_4$/N$_2$H$_4$PhCl. The resulting data were used to calculate the acid dissociation (pK_a) constants corresponding to N$_2$H$_4$X$^+$, **1**–**8** and adducts of both, and the metal hydrolysis (pK_{OH}) constants of the last two systems. The titration data at pH > 10 in the case of **1**–**8** and at pH > 9.0 in the case of N$_2$H$_4$X$^+$ adducts were not considered in the present investigations. The acid dissociation constants of N$_2$H$_4$X$^+$ and the unco-ordinated COOH/CH$_2$CH$_2$OH in complexes **1**–**8** and

in their 1:1 adducts of $N_2H_4X^+$, where the dissociation of protons takes place in well defined buffer regions, were evaluated[29] with the help of K_w (1.008×10^{-14} at 25 °C) and suitable mass and charge balance equations fitting to the generalized eqn. (1).

$$H_nL \xrightarrow{K_{na}} H_{n-1}L + H^+$$

$$K_{na} = [H_{n-1}L][H^+]/[H_nL] \qquad (1)$$
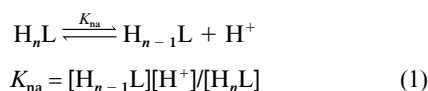
Charges on the species are omitted for the sake of clarity. The stepwise first, second or third metal hydrolyses of **1**–**8** and their $N_2H_4X^+$ adducts were considered according to reactions (2).

$$M(OH)_{n-1} + H_2O \xrightarrow{K_{OH}} M(OH)_n + H^+$$

$$K_{OH} = [M(OH)_n][H^+]/[M(OH)_{n-1}] \qquad (2)$$
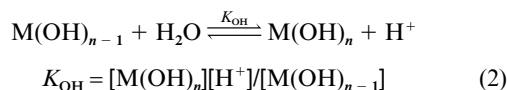
The hydrolysis constants falling in the pH range 2 < pH < 10 were calculated with the help of suitable mass balance equations and K_w at 25 °C.

A graphical method[30] was used to calculate the dissociation constants, in the case of simultaneous dissociation of two protons (either by the participation of $COOH/CH_2CH_2OH$ and/or in the combination of dissociation of $N_2H_4X^+$ proton and metal hydrolysis) described by the generalized eqn. (3) or combined eqns. (1) and (2), respectively.

$$H_2L \xrightarrow{K_a, K_{2a}} L + 2H^+$$

$$K_aK_{2a} = [L][H^+]^2/[H_2L] \qquad (3)$$
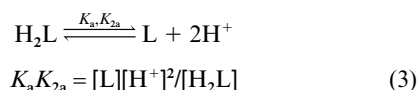
The absorption spectral studies on complexes **1**–**8** (1 mM) in the absence and in the presence of various concentrations of $N_2H_5^+$ or $N_2H_4Ph^+$ (1–100 mM) were performed at pH 2.8 in a 10 mm quartz cuvette and the spectra were recorded in the wavelength range between 200 and 700 nm at 25 ± 0.1 °C.

The voltammetric responses were recorded with a weighed quantity of complex (1 mM) in the absence or presence of a known concentration (0.1–100 mM) of substrate ($N_2H_5^+$/$N_2H_4Ph^+$) in 10 mL electrolyte solution at the desired pH under Ar at 25 °C. The *i vs. E* plots were recorded between +0.2 and −0.8 V (*vs.* SCE) at the sweep rates 10 mV s^{-1} in sampled dc and 20–500 mV s^{-1} in cyclic voltammetry (CV). The effect of pH on the diffusion current (i_d) and half-wave potentials ($E_{1/2}$) was studied in the range 1–5. All the solutions were deaerated at least 15 min prior to measurements and the experiments were maintained at 25 ± 0.1 °C unless otherwise stated. The criteria for the electrochemical reversibility and diffusion current were established by following the reported techniques.[31,32]

Constant potential electrolysis was performed in 25 mL of deaerated buffer solution having the desired pH (1.9/2.8) containing 1 mmol of complex (**1**–**8**) and 100 mmol of substrate at predetermined potential for at least 10 h under Ar at 25 ± 0.1 °C. The ammonia produced during the reaction was estimated every hour[21] while the aniline produced concomitantly with ammonia was tested qualitatively using vanadium(v) salt.[33]

Results and discussion

Interaction of $N_2H_4X^+$ with the complexes 1–8

Potentiometry. Complexes **1**–**8** were independently titrated against standard sodium hydroxide in the absence and in the presence of one equivalent of $N_2H_4X^+$. The representative titration data thus obtained with **1** are presented in Fig. 1. Complex **1** (Fig. 1(a)) showed three titratable protons dissociating in three independent buffer regions, two in acidic and one in basic pH by the metal hydrolysis. Further hydrolysis of **1** occurring beyond a > 3 resulted in a dark brown solution which
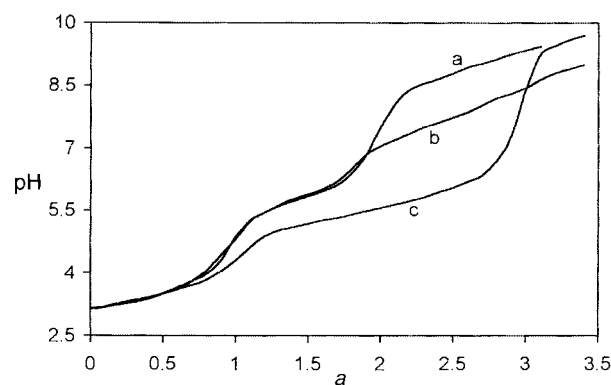
Fig. 1 Potentiometric titration curve of (a) $K_2[Ru(imda)Cl_3]\cdot 2H_2O$, 1 mM; (b) $K_2[Ru(imda)Cl_3]\cdot 2H_2O$, 1 mM and $N_2H_5^+$, 1 mM; (c) $K_2[Ru(imda)Cl_3]\cdot 2H_2O$, 1 mM and $N_2H_4Ph^+$, 1 mM at 25 °C. $I = 0.1$ M (Na_2SO_4), a = mols of base added per mol of complex or $N_2H_4X^+$.

may be due to its decomposition and hence was not considered here. Similarly, complexes **2** and **3** showed three buffer regions caused by metal hydrolyses at 2 < pH < 10 with two ill defined inflections at a = 1 and 2. On the other hand, **4**–**7** showed the stepwise liberation of two protons in two well defined buffer regions 0 < a < 1 and 1 < a < 2. Of the two, the first buffer region is assigned to the dissociation of an unco-ordinated CO_2H proton in the case of complexes **5**–**7** and may be the OH (CH_2CH_2OH) proton in the case of **4** while the second buffer region is considered for the metal hydrolysis.[33,34] On the contrary, the complex **8** showed one buffer region 0 < a < 2 in acidic pH followed by another buffer region 2 < a < 3 in basic pH. The first buffer region is assigned to the simultaneous liberation of two protons on the dtpa ligand, the second to metal hydrolysis.

The metal hydrolysis steps, three in the case of complex **1**, the first two in the case of **2** and **3**, the single one in the case of **4**–**6** and **8**, and the first one in the case of **7**, are accounted for by the rapid substitution of chloride ions by H_2O as verified kinetically in the case of **4**–**6**, and the liberation of titratable protons following its dissociation.[26,35] The third metal hydrolysis step in the case of **2** and **3** could be explained if one of the loosely bound carboxylate groups of the tetradentate himda and nta is substituted by H_2O or the liberation of OH (CH_2CH_2OH) proton on tridentate himda in **2**. The acid (pK_a) and metal hydrolysis (pK_{OH}) constants were calculated with the help of eqns. (1)–(3) and are given in Table 1. These showed that the complexes **1**–**3** are more hydrolysable because the chelation capability of imda (tri), himda (tri or tetra) and nta (tetra) ligands is low. All other complexes, **4**–**8**, showed a single hydrolysis step which occurs almost at neutral pH. This implies that all these complexes have a potential site available to another ligand for co-ordination/substitution, though the number of co-ordinating sites in the aminopolycarboxylic acid ligand varies from 5 to 8. The present data also revealed that only five co-ordination sites on the hexacovalent ruthenium are used by all penta- or higher poly-dentate aminopolycarboxylic acids in the process of bond formation. The hydrolytic tendency of the metal increased in the order **8 < 4 < 5 < 6 < 7 < 2 < 3 < 1**.

The titration data of $N_2H_5HSO_4$ showed two buffer regions separated by an inflection at a = 1. The buffer region 0 < a < 1 is considered for the neutralization of the strong acidic proton due to the HSO_4^- group, since the $N_2H_6^{2+}$ (K_a 11)[11] does not form inder the present experimental conditions. The buffer region corresponding to this proton was ignored in all other studies presented below and hence not included in Fig. 1(b), but considered in the evaluation of relevant constants. The second buffer region 1 < a < 2 is assigned to the neutralization of proton in the equilibrium $N_2H_5^+ \rightleftharpoons N_2H_4 + H^+$. Similarly, the titration data of N_2H_4PhCl contained a single buffer region

Table 1 Acid dissociation (pK_a) and metal hydrolysis (pK_{OH}) constants of complexes **1**–**8** at 25 °C, $I = 0.1$ M (Na$_2$SO$_4$)

| Complex | pK_a | | pK_{OH} | | |
	CO$_2$H	CH$_2$CH$_2$OH	First	Second	Third
1	—	—	2.42 ± 0.02	5.78 ± 0.03	8.86 ± 0.03
2	—	—	2.86 ± 0.02	5.72 ± 0.02	8.53 ± 0.03
3	—	—	2.47 ± 0.01	4.80 ± 0.03	9.62 ± 0.03
4	—	4.82 ± 0.03	7.96 ± 0.03	—	—
5	2.34 ± 0.02	—	7.64 ± 0.02	—	—
6	2.38 ± 0.02	—	7.60 ± 0.02	—	—
7	2.55 ± 0.03	—	6.20 ± 0.03	—	—
8	(2.58, 3.40)	—	8.28 ± 0.02	—	—

Values given in parentheses were evaluated by a graphical method.

Table 2 Acid dissociation (pK_a) and metal hydrolysis (pK_{OH}) constants of N$_2$H$_4$X$^+$ and their adducts with complexes **1**–**8** at 25 °C, $I = 0.1$ M (Na$_2$SO$_4$)

| Adduct | | pK_a | | pK_{OH} | |
N$_2$H$_4$X$^+$	Complex	N$_2$H$_4$X$^+$	CO$_2$H/CH$_2$CH$_2$OH	First	Second
N$_2$H$_5^+$	—	8.05 ± 0.01	—	—	—
	1	7.67 ± 0.02	—	2.43 ± 0.02	5.82 ± 0.03
	2	7.42 ± 0.03	—	2.82 ± 0.02	—
	3	7.36 ± 0.02	—	2.45 ± 0.02	—
	4	7.65 ± 0.02	4.83 ± 0.02	—	—
	5	7.52 ± 0.02	2.40 ± 0.02	—	—
	6	7.28 ± 0.03	2.42 ± 0.02	—	—
	7	7.15 ± 0.02	2.58 ± 0.02	—	—
	8	7.30 ± 0.03	(2.60, 3.43)	—	—
N$_2$H$_4$Ph$^+$	—	5.27 ± 0.02	—	—	—
	1	(5.24)	—	2.45 ± 0.02	(5.84)
	2	5.25 ± 0.02	—	2.89 ± 0.03	—
	3	5.34 ± 0.02	—	2.50 ± 0.03	—
	4	(5.32)	(4.62)	—	—
	5	5.20 ± 0.02	2.35 ± 0.02	—	—
	6	5.22 ± 0.02	2.41 ± 0.02	—	—
	7	5.31 ± 0.02	2.60 ± 0.02	—	—
	8	5.30 ± 0.02	(2.64, 3.49)	—	—

Values given in parentheses were evaluated by a graphical method.

$0 < a < 1$, representing the equilibrium N$_2$H$_4$Ph$^+ \rightleftharpoons$ N$_2$H$_3$Ph + H$^+$.

The titration curves of complexes **1**–**8** in the presence of N$_2$H$_5^+$ possessed buffer regions, four in the case of **1** (Fig. 1(b)) and three in the case of **2**–**8**. The last buffer region (fourth in the case of **1**, and third in the case of other complexes), where Ru^{III}–N$_2$H$_5^+$ species were decomposed to give ruthenium(II) complexes, as found by sampled dc at pH > 9, was not considered in the present study. The third buffer region in the case of **1** and the second in the case of **2**–**8**, which were assigned earlier to metal hydrolysis in the absence of N$_2$H$_5^+$, are assigned to the equilibrium N$_2$H$_5^+ \rightleftharpoons$ N$_2$H$_4$ + H$^+$ in the vicinity of the metal co-ordination sphere. The first and second buffer regions in the case of **1** and the first in the case of **2** and **3** are assigned to the metal hydrolysis, while the first in the case of **4**–**7** and the first and second buffer regions in the case of **8** are assumed for the deprotonation of the CO$_2$H/CH$_2$CH$_2$OH group on the aminopolycarboxylic acid as found above in the absence of N$_2$H$_5^+$.

The potentiometric data obtained in the presence of N$_2$H$_4$PhCl showed two buffer regions: $a = 0$–1, 1–3 in the case of complex **1** (Fig. 1(c)), $a = 0$–1, 1–2 in the case of **2**, **3** and **5**–**7** and $a = 0$–2, 2–3 in the case of **8**, while one buffer region $a = 0$–2 in the case of **4**. It was noticed that the hydrolysis steps, third in the case of **1**, second in the case of **2** and **3**, and first in the case of **5**–**8** which were observed in the absence of N$_2$H$_4$Ph$^+$, were not seen. Thus, the deprotonation of N$_2$H$_4$Ph$^+$ was assumed in the buffer region $a = 1$–3 in the presence of **1** along with the second metal hydrolysis, 1–2 in the presence of **2**, **3**, **5**–**7**, 0–2 in the case of **4** together with the deprotonation of the OH (CH$_2$CH$_2$OH) proton and 2–3 in the case of **8**.

The acid dissociation constants and metal hydrolysis constants corresponding to free N$_2$H$_4$X$^+$ and its adducts with complexes **1**–**8** were calculated with the help of eqns. (1)–(3) and presented in Table 2. The values of K_a (CO$_2$H/CH$_2$CH$_2$OH) and K_{OH} are closely comparable to the corresponding values seen in Table 1. Moreover, the values obtained for N$_2$H$_4$X$^+ \rightleftharpoons$ N$_2$H$_3$X + H$^+$ in the presence of **1**–**8** are in close agreement with those obtained in their absence. However, the K_a value is reduced to only 0.38–1.0 logarithmic units in the case of N$_2$H$_5^+$ and negligibly affected in the case of N$_2$H$_4$Ph$^+$ after their interaction with the ruthenium complex. On the basis of these observations together with the disappearance of metal hydrolysis steps (third in the case of **1**, second in the of **2** and **3**, and first in the other complexes as seen in Table 1) in the presence of N$_2$H$_4$X$^+$, the co-ordination of N$_2$H$_4$X$^+$ to ruthenium occurs at the vacant site where the poorly dissociable water was attached. Further, the small changes in pK_a values of the N$_2$H$_4$X$^+$ ligand after its interaction with ruthenium suggests that its co-ordination takes place through the weakly basic nitrogen (NH$_2$ of N$_2$H$_5^+$ or NHPh of N$_2$H$_4$Ph$^+$) leaving the other nitrogen in the protonated form, which is further confirmed by the voltammetric data presented at pH < 3.0 in the latter part of this paper.

Absorption spectra. The electronic absorption spectra of complexes **1**–**8** were recorded under identical conditions in the absence and presence of N$_2$H$_4$X$^+$ salts at different compositions at pH 2.8 to verify the interaction of the latter (N$_2$H$_4$X$^+$) through the weakly basic nitrogen with ruthenium. In the absence of N$_2$H$_4$X$^+$ the ligand charge transfer between 240 and

Table 3 Absorption spectral data of complexes **1–8** in the absence and in the presence of $N_2H_4X^+$ at pH 2.8

| Complex | λ_{max}/nm (ε_{max}/M^{-1} cm^{-1}) | | |
	Absence	Presence of $N_2H_5^+$	Presence of $N_2H_4Ph^+$
1	240(2270); 285(1400); 365(445)	240(2240); 285(1340)	420(1070); 540(350)
2	245(2595); 285(2360); 360(640)	245(2370); 285(2320)	425(1450); 540(350)
3	245(2330); 285(2200); 360(735)	245(2290); 285(2120)	420(1360); 540(350)
4	240(2270); 285(1400); 360(445)	240(2240); 285(1375)	400(1400); 540(260)
5	245(2600); 285(2370); 360(640)	245(2570); 285(2360)	420(2250); 540(480)
6	245(2565); 285(2420); 360(630)	245(2560); 285(2380)	400(1350); 540(130)
7	240(2430); 285(1630); 360(700)	240(2390); 285(1580)	430(1230)
8	235(2240); 280(1560); 360(375)	235(2230); 280(1540)	450(1270)

Table 4 Half wave potentials of the Ru^{III} ⟶ Ru^{II} wave and those of complexes **1–8** observed in the presence of 100 equivalents of $N_2H_4X^+$ at pH 2.8

| Complex | $-E_{1/2}$/V *vs.* SCE | | |
	Absence	Presence of $N_2H_5^+$	Presence of $N_2H_4Ph^+$
1	0.372	0.346, 0.475	0.360, 0.482
2	0.364	0.328, 0.450	0.340, 0.462
3	0.354	0.300, 0.440	0.322, 0.456
4	0.248	0.030, 0.256	0.165, 0.248, 0.335
5	0.238	0.025, 0.230	0.150, 0.225, 0.346
6	0.251	0.034, 0.250	0.156, 0.235, 0.340
7	0.286	0.045, 0.230	0.168, 0.260, 0.386
8	0.165	0.028, 0.250	0.154, 0.250, 0.395
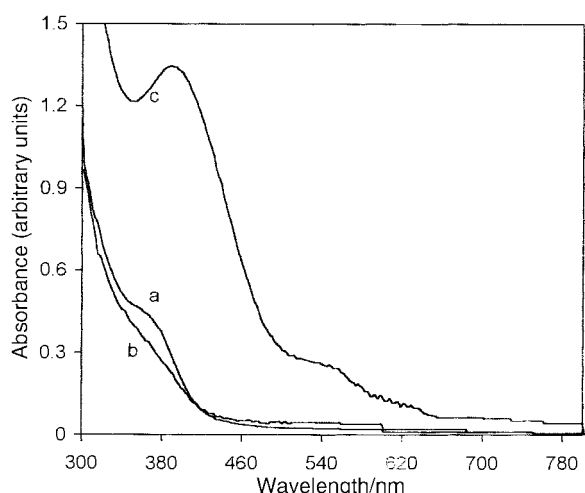
Fig. 2 Absorption spectra of (a) K[Ru(hedta)Cl], 1 mM; (b) K[Ru(hedta)Cl], 1 mM and $N_2H_5^+$, 1 mM; (c) K[Ru(hedta)Cl], 1 mM and $N_2H_4Ph^+$, 1 mM. In all cases the pH was 2.8.

Fig. 3 Sampled dc polarogram of (a) $K_2[Ru(imda)Cl_3]\cdot 2H_2O$, 1 mM; (b) $K_2[Ru(imda)Cl_3]\cdot 2H_2O$, 1 mM and $N_2H_5^+$, 100 mM; (c) $K_2[Ru(imda)Cl_3]\cdot 2H_2O$, 1 mM and $N_2H_4Ph^+$, 100 mM. The pH in each case was maintained at 2.8.

250 nm and the ligand to metal charge transfer bands in the regions 280–290 and 360–370 nm were observed for all complexes. The absorption band at 360 nm, characteristic of a Ru–OH$_2$ bond,[36] was reduced in intensity on introduction of $N_2H_5^+$ due to the replacement of bound water molecule by the latter. In the case of addition of $N_2H_4Ph^+$ two new absorption bands at 400–450 and 540 nm appeared rapidly. The band at 540 nm did not occur in the case of complexes **7** and **8**. Concomitantly, the yellow colour of these complexes instantly changed to reddish brown accounting for the formation of $N_2H_4Ph^+$ adducts in solution. Further, plots of change in absorbance (Δ*A*) *vs.* the ratio [$N_2H_4X^+$]:[complex] confirmed the formation of 1:1 $N_2H_4X^+$ adducts as suggested above with **1–8**. Fig. 2 shows the typical spectral changes observed with **4** in the absence and in the presence of $N_2H_4X^+$ (1 mM) at pH 2.8. The spectral features observed with all complexes **1–8** are summarized in Table 3.

Voltammetry. Sampled dc polarograms of complexes **1–8**

were recorded in the absence and in the presence of various equivalents of $N_2H_4X^+$. In the absence, each complex exhibited a well defined one-electron cathodic wave in the potential range between -0.150 and -0.400 V ($E_{1/4} - E_{3/4}$ 55–65 mV; *I* (diffusion current constant) 1.2–1.5) *vs.* SCE assignable to the Ru^{III} ⟶ Ru^{II} process. The height of this wave proportionately enhanced with increase in complex concentration, while the plots E_{de} (potential at the electrode) *vs.* log [$i/(i_d - i)$] were linear with a slope of about 70 mV, indicating the electrode reactions are one-electron, diffusion controlled and quasi-reversible processes. The wave shifted to a measurable extent (60 mV per pH unit) in the case of **1–3**, less in the case of other complexes with the change in pH between 1.0 and 5.0. The polarogram of **1** representing this one-electron wave is shown in Fig. 3(a) while the half-wave potential ($E_{1/2}$) data of all the complexes **1–8** are listed in Table 4. It decreased in the order **8 > 5 > 4 > 6 > 7 > 3 > 2 > 1** which is in good agreement with the order of sigma basicity of the co-ordinated aminopolycarboxylic acid.[37] However, it is noted that the $E_{1/2}$ values for **1–3** are relatively more negative than those of other complexes. This may be attributed to the strong hydrolytic tendency of these complexes when dissolved in aqueous solution. Accordingly, the hydrolytic tendency of these complexes may be given as **3 < 2 < 1**. On the other hand, the lower $E_{1/2}$ value for complex **8** than those of **4–7** may be accounted for by its destabilization due to steric repulsion because of the large size of dtpa, despite its large sigma basicity.

When 0.1–5.0 equivalents of $N_2H_5^+$ were introduced into the complex solution the $Ru^{III} \longrightarrow Ru^{II}$ wave was enhanced while its plateau extended to anodic potentials in cases of complexes **1–8**. As a result, the $E_{1/2}$ value apparently shifted to anodic potentials. A plot of the enhanced current increased linearly as the number of equivalents of added $N_2H_5^+$ approached unity and remained constant thereafter indicating the instant formation of monomeric $N_2H_5^+$ complexes in acidic solutions, as suggested above. The plateau of the enhanced wave gradually split into two as $[N_2H_5^+]$ reached twenty times more than that of the complex and the wave finally appeared as two distinguishable waves (w_1 and w_2) at all other compositions of $N_2H_5^+$. The polarographic responses of **1** in the presence of 100 equivalents of $N_2H_5^+$ are shown in Fig. 3(b). In all cases, the wave w_1 ($E_{1/4} - E_{3/4}$ 32 mV; I 1.9) shifted anodically with the increase in $[N_2H_5^+]$ while the wave w_2 ($E_{1/4} - E_{3/4}$ 65 mV; I 1.0) remained steady. On the other hand, the diffusion currents of w_1 and w_2 were directly proportional to [complex]. The plots E_{de} vs. log $[i/(i_d - i)]$ for w_1 and w_2 were linear with slopes of 33 and 68 mV, respectively. The diffusion current (i_d) of the composite wave or of the wave w_1 or w_2 was maximum in the pH range 2.5–3.5 and somewhat reduced when the ionic strength was raised beyond 0.5 M. Besides, the wave w_1 shifted negligibly with increase in pH between 1 and 4. The $E_{1/2}$ data (Table 4) revealed that the wave w_1 is 0.02–0.05 V less negative in the case of **1–3**, while it is 0.13–0.22 V less negative in the case of **4–8** compared to that of the corresponding one-electron $Ru^{III} \longrightarrow Ru^{II}$ wave observed before the addition of $N_2H_5^+$. Similarly, the wave w_2 is about 0.09–0.10 V more negative in the case of **1–3** and **8** and similar in the case of **4–7** to that of the initial one-electron $Ru^{III} \longrightarrow Ru^{II}$ wave. The wave w_1 in the case of **1–3** is more negative than that of the complexes **4–7**. The $E_{1/2}$ of w_1 is correlated with ΣpK_a of the primary ligand,[37] aminopolycarboxylic acid. The large negative $E_{1/2}$ for complexes **1–3** is responsible for their hydrolytic tendency, while the negligible dependence of $E_{1/2}$ in complexes **4–8** shows that there is no considerable change in the redox properties of the metal with the increase in sigma basicity of the aminopolycarboxylic acid. Probably, this could be due to identical binding of penta-, hexa- or hepta-dentate aminopolycarboxylic acids to ruthenium through the same number of co-ordinating groups.

The polarographic responses of complex **1** in the presence of 0.1–100 equivalents of $N_2H_4Ph^+$ were probed. The response in 100 equivalents of $N_2H_4Ph^+$ is depicted in Fig. 3(c). It displayed two closely separated waves (w_1 and w_2) at potentials close to that of the $Ru^{III} \longrightarrow Ru^{II}$ wave with a doubled diffusion current. The responses in the presence of other concentrations (0.1–100 equivalent of $N_2H_4Ph^+$) overlapped those in Fig. 3(c) except for a negligible negative shift in $E_{1/2}$ and a minor change in the overall diffusion current. Complexes **2** and **3** also exhibited two cathodic waves replacing the $Ru^{III} \longrightarrow Ru^{II}$ wave while the other complexes (**4–8**) showed an additional low intensity wave poorly resolved from w_1 and w_2. The $E_{1/2}$ data pertaining to these waves are summarized in Table 4. The measured data ($E_{1/4} - E_{3/4}$ 34 mV and I 2.0 for w_1; 65 mV and 0.9 for w_2) indicated w_1 to be a two-electron process while w_2 and the additional wave are one-electron processes. This was further substantiated by plots of E_{de} vs. log $[i/(i_d - i)]$ which were linear having slopes of 32–35 mV for w_1 and 67–70 mV for both w_2 and the additional wave. The overall diffusion current at -0.5 V was proportional to [**1**] while the enhanced current (Δi_d) was a maximum in the pH range 2.0 to 3.5. The data in Table 4 revealed that, for a given complex, the $E_{1/2}$ of both w_1 and w_2 are more negative with $N_2H_4Ph^+$ than with $N_2H_5^+$, indicating that the former hydrazine binds to ruthenium more strongly than the latter can through a sigma bond. This may due to the effect of phenyl ring substitution on the co-ordinating nitrogen in the former hydrazine. The $E_{1/2}$ values of w_1 obtained with complexes **1–8** in the presence of $N_2H_4Ph^+$ are correlated with ΣpK_a of the aminopolycarboxylic acid[37] attached
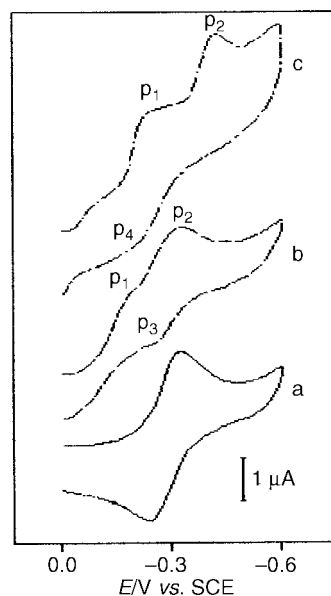

Fig. 4 Cyclic voltammograms of (a) $K[Ru(Hcdta)Cl]\cdot H_2O$, 1 mM; (b) $K[Ru(Hcdta)Cl]\cdot H_2O$, 1 mM and $N_2H_5^+$, 100 mM; (c) $K[Ru(Hcdta)Cl]\cdot H_2O$, 1 mM and $N_2H_4Ph^+$, 100 mM. The pH in each case was maintained at 2.8.

to ruthenium. Again, the large negative values in the case of **1–3** and negligible dependence of $E_{1/2}$ in the case of **4–8** are accounted for by the reasons given before.
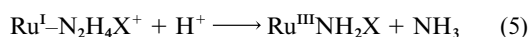
The CV responses of complexes **1–8** in the absence and in the presence of $N_2H_4X^+$ were run subsequently for the above solutions. The results in the absence and in the presence of 100 equivalents of $N_2H_4X^+$ are discussed below. All the complexes, in the absence of $N_2H_4X^+$, yielded a pair of cathodic and anodic peaks corresponding to the quasi-reversible Ru^{III}–Ru^{II} couple. Fig. 4(a) shows a typical cyclic voltammogram of **4**, which peaked at -0.320 V in the forward scan and at -0.252 V in the reverse scan. The peak separation which varied between 70 and 65 mV at 0.1 V s^{-1} increased with increase in scan speed, while the peak width $E_{p/2} - E_p$ tended to 62–65 mV which is close to the theoretical value for a one-electron process. On the other hand, the peak currents increased linearly with increase in the square root of the scan speed, while the peak to peak ratio ($i_{pa} : i_{pc}$) was less than unity.

All the complexes, in the presence of 100 equivalents of $N_2H_5^+$, exhibited two well resolved cathodic peaks (p_1 and p_2 corresponding to the polarographic waves w_1 and w_2, respectively) and a single anodic peak (p_3, counterpart of p_2). The anodic counterpart of p_1 did not appear under the present experimental conditions. Representative CV responses of complex **4** are shown in Fig. 4(b). The complexes **1–3** exhibited two well resolved cathodic peaks (p_1 and p_2) in the presence of 100 equivalents of $N_2H_4Ph^+$. Contrarily, they showed a single anodic peak (p_4) as counterpart of p_1 and no peak for p_2. Complexes **4–8** behaved similarly in the presence of 100 equivalents of $N_2H_4Ph^+$. Additionally, they showed a well defined cathodic peak and its counterpart (Fig. 4(c)) corresponding to the additional wave observed in sampled dc between w_1 and w_2. The peak analyses data for p_1 and p_2, confirmed them to be a two- and one-electron reduction process, respectively. Peak p_1 shifted anodically with increase in $[N_2H_4X^+]$ but cathodically with increase in scan speed, but plots of i_{pc} vs. $v^{1/2}$ were linear for both p_1 and p_2.
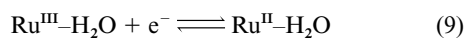
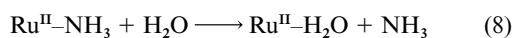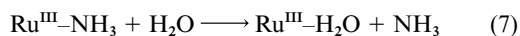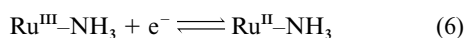## Mechanism of electrode reactions

The complexes **1–8** were reduced in solution in the absence and in the presence of one equivalent of $N_2H_4X^+$ at pH 1.9 and 2.8 by holding the potential at a mercury pool cathode at 0.1 V away from the $E_{1/2}$ of $Ru^{III} \longrightarrow Ru^{II}$ wave as given in Table 4. In
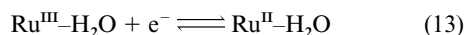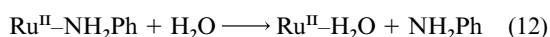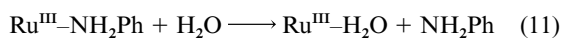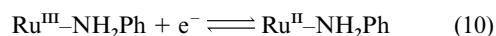
the absence, all the complexes consumed one faraday of charge and produced the corresponding ruthenium(II) complexes. In the presence of $N_2H_4X^+$ all the complexes consumed three faradays. The electrolysed solutions contained an ammonia concentration two times that of $[N_2H_5^+]$ but equal to that of $[N_2H_4Ph^+]$ taken initially. On the basis of these data and the data in Figs. 3 and 4, it is proposed that the Ru^{III}–$N_2H_4X^+$ complexes take two electrons from the electrode at w_1 and produce Ru^I–$N_2H_4X^+$ species (reaction (4), charges on the species

$$Ru^{III}\text{–}N_2H_4X^+ + 2e^- \rightleftharpoons Ru^I\text{–}N_2H_4X^+ \qquad (4)$$

$$Ru^I\text{–}N_2H_4X^+ + H^+ \longrightarrow Ru^{III}NH_2X + NH_3 \qquad (5)$$

When X = H

$$Ru^{III}\text{–}NH_3 + e^- \rightleftharpoons Ru^{II}\text{–}NH_3 \qquad (6)$$

$$Ru^{III}\text{–}NH_3 + H_2O \longrightarrow Ru^{III}\text{–}H_2O + NH_3 \qquad (7)$$

$$Ru^{II}\text{–}NH_3 + H_2O \longrightarrow Ru^{II}\text{–}H_2O + NH_3 \qquad (8)$$

$$Ru^{III}\text{–}H_2O + e^- \rightleftharpoons Ru^{II}\text{–}H_2O \qquad (9)$$

When X = Ph

$$Ru^{III}\text{–}NH_2Ph + e^- \rightleftharpoons Ru^{II}\text{–}NH_2Ph \qquad (10)$$

$$Ru^{III}\text{–}NH_2Ph + H_2O \longrightarrow Ru^{III}\text{–}H_2O + NH_2Ph \qquad (11)$$

$$Ru^{II}\text{–}NH_2Ph + H_2O \longrightarrow Ru^{II}\text{–}H_2O + NH_2Ph \qquad (12)$$

$$Ru^{III}\text{–}H_2O + e^- \rightleftharpoons Ru^{II}\text{–}H_2O \qquad (13)$$

are omitted for clarity). These ruthenium(I) species are less stable and hence rapidly decompose as shown in reaction (5) to Ru^{III}–NH_2X and one mole of NH_3 by abstracting one equivalent of H^+ from the medium. The species Ru^{III}–NH_2X are reduced by one electron in a subsequent step at w_2 (reactions (6) and (10)) to give Ru^{II}–NH_2X which on aquation produces the corresponding Ru^{II}–H_2O species and NH_2X (reactions (8) and (12)), or hydrolyse to Ru^{III}–OH_2 producing an equivalent amount of NH_2X (reactions (7) and (11)). The Ru^{III}–OH_2 species thus produced may be reduced along with Ru^{III}–NH_2X at w_2 in the case of $N_2H_5^+$ (reaction (9)) or at potentials where a new reduction step appeared between w_1 and w_2 in the case of $N_2H_4Ph^+$ (reaction (13)). The Ru^{II}–NH_2Ph complexes produced at w_1 are not as stable as the corresponding Ru^{III}–NH_3 due to the presence of the Ph group and hence these species and their reduced forms Ru^{II}–NH_2Ph quickly hydrolyse to the corresponding aqua species and NH_2Ph (reactions (11) and (12)). This may be the reason for the irreversible nature of wave w_2 and reversible nature of the poorly resolved new wave between w_1 and w_2.

Electrolytic reduction of $N_2H_4X^+$ in the presence of complexes 1–8

The hydrazines $N_2H_4X^+$ were electrolytically reduced at pH 1.9 and 2.8 under Ar by constant potential coulometry by holding the potential at 50 mV away from the corresponding $E_{1/2}$ of w_1 given in Table 5 in order to measure the catalytic ability of the ruthenium as a function of the sigma basicity of the amino-polycarboxylic acid on the reduction of the N–N bond in $N_2H_4X^+$. In all cases the constant reduction of $N_2H_4X^+$ to NH_3 and NH_2X occurred, eqn. (14), justifying the wave w_1 as a multi-electron process.

$$N_2H_4X^+ + 2e^- + H^+ \xrightarrow{\ Ru^{III}\text{–}N_2H_4X^+\ } NH_3 + NH_2X \qquad (14)$$
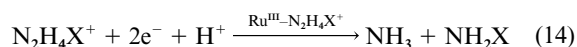
At both pH studied, the number of mols of NH_3 produced per mol of complex was linear, in all cases, as seen in Fig. 5 for
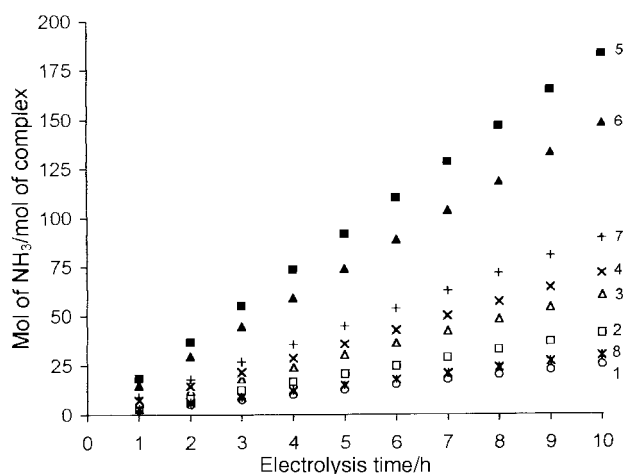

Fig. 5 Plots of mols of NH_3 produced per mol of complex (**1–8**) during the reduction of $N_2H_5^+$ at pH 2.8 *vs.* electrolysis time.
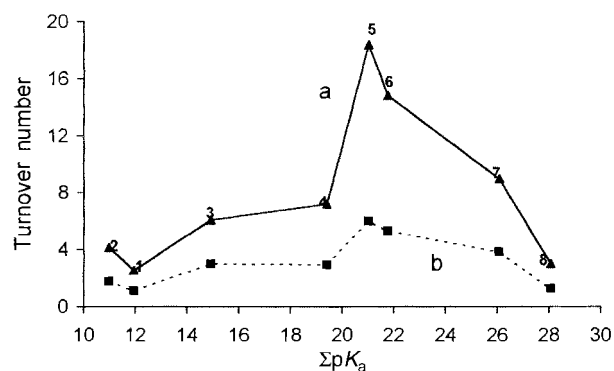

Fig. 6 Plot of turnover number of NH_3 produced by the reduction of $N_2H_4X^+$ *vs.* ΣpK_a of the aminopolycarboxylic acid: (a) $N_2H_5^+$, (b) $N_2H_4Ph^+$.

$N_2H_5^+$ reduction. The turnover number and mols of NH_3 formed per mol of complex per hour are given in Table 5. For a given substrate, the turnover number at pH 2.8 is nearly double that at pH 1.9. The observed turnover number of NH_3 obtained with $N_2H_4Ph^+$ is less than half of that achieved with $N_2H_5^+$. However, the coulombic efficiency in all these cases was almost 100%. The solution at the end of electrolysis showed the same voltammetric features as described above and produced NH_3 at the same turnover rate when an additional amount of $N_2H_4X^+$ was added to the electrolysed solution and the electrolysis continued after adjusting the pH to the initial value. Thus, the catalytic efficiency of the metal was shown to be intact during the reduction cycle.

The turnover rate is correlated in Fig. 6 with the sigma basicity of the polyaminopolycarboxylic acid. The data revealed that the turnover rate increases with the increase in sigma basicity of the aminopolycarboxylic acid to nearly $\Sigma pK_a = 22$ and then decreases thereafter. With the given hydrazine $N_2H_5^+/N_2H_4Ph^+$, it increases in the order $1 < 2 < 3 < 4 < 5 \approx 6$ as the sigma basicity of the aminopolycarboxylic acid increases in the order $2 < 1 < 3 < 4 < 5 < 6$. The lower turnover rate for complex **1** than that of **2** is explained by its high hydrolytic tendency. The decrease in the turnover rate with **5–8** with the increase in the sigma basicity may be related to the structural constraints developed within the aminopolycarboxylic acid due to increase in size, affecting the overall catalytic ability of the ruthenium.

Conclusion

Ruthenium(III)–aminopolycarboxylic acid complexes of tri- (imda, himda), tetra- (himda, nta), penta- (hedtra), hexa- (edta, pdta and cdta) and octa- (dtpa) dentate ligands were prepared

Table 5 Turnover number, moles of NH_3 produced per mol of complex per hour, during the reduction of $N_2H_4X^+$

	Turnover number					
	$N_2H_5^+$			$N_2H_4Ph^+$		
Complex	Potential/V	pH 1.9	pH 2.8	Potential/V	pH 1.9	pH 2.8
1	−0.350	1.44	2.54	−0.400	0.94	1.10
2	−0.200	1.76	4.12	−0.300	1.02	1.76
3	−0.350	2.98	6.06	−0.400	1.78	2.98
4	−0.200	3.75	7.18	−0.250	1.62	2.95
5	−0.050	9.50	18.40	−0.200	2.85	5.98
6	−0.100	7.96	14.84	−0.220	2.68	5.32
7	−0.175	4.46	8.98	−0.300	2.17	3.84
8	−0.100	1.34	2.95	−0.230	0.92	1.27

and characterized. Interaction of these complexes with hydrazines $N_2H_4X^+$ (X = H or Ph) was investigated by pH-metry, voltammetry and spectrophotometry. The results confirmed that these complexes rapidly form monomeric adducts with $N_2H_4X^+$ by its substitution at the less hydrolysable metal co-ordination site in acidic media. These adducts readily accept two electrons to form the corresponding $Ru^I–N_2H_4X^+$ which on decomposition give one mol of ammonia and an electroactive species which in a subsequent chemical step gives one mol of NH_2X. Employing these hydrazinium adducts, $N_2H_4X^+$ were reduced electrolytically. Ammonia and/or amine was obtained in catalytic amounts with nearly 100% coulombic efficiency. The turnover rate of ammonia produced per mol of complex per hour was evaluated and correlated with the sigma basicity (ΣpK_a) of the aminopolycarboxylic acid. The data revealed that the turnover rate increased with increase in sigma basicity in the order imda < himda < nta < hedtra < edta ≈ pdta. Further increase in the sigma basicity of the aminopolycarboxylic acid reduced the catalytic ability of the ruthenium which is attributed to the development of complexity caused by the concomitant increase in size of the aminopolycarboxylic acid. The most probable chemical and charge transfer steps were suggested for the reactions at the electrode.

Acknowledgements

References

1 H. Dalton and L. E. Mortenson, *Bacteriol. Rev.*, 1972, **21**, 29.
2 J. Chatt, J. R. Dilworth and R. L. Richards, *Chem. Rev.*, 1978, **78**, 589; P. Pelikan and R. Boca, *Coord. Chem. Rev.*, 1984, **55**, 55.
3 R. A. Handerson, G. J. Leigh and C. J. Pickett, *Adv. Inorg. Chem. Radiochem.*, 1983, **27**, 198.
4 B. K. Burgess and D. J. Lowe, *Chem. Rev.*, 1996, **96**, 2983; J. B. Howard and D. C. Rees, *Chem. Rev.*, 1996, **96**, 2965.
5 D. Sellmann and J. Sutter, *Acc. Chem. Res.*, 1997, **30**, 460.
6 B. E. Smith, M. C. Durrant, S. A. Fairhurst, C. A. Gormal, K. L. C. Gornburg, R. A. Henderson, S. K. Ibrahim, T. Le. Gall and C. J. Pickett, *Coord. Chem. Rev.*, 1999, **185–186**, 669.
7 R. N. F. Thorneley, R. R. Eady and D. J. Lowe, *Nature* (*London*), 1978, **272**, 557.
8 B. T. Heaton, C. Jacob and P. Page, *Coord. Chem. Rev.*, 1996, **154**, 193 and references therein.
9 P. B. Hitchcock, D. L. Hughes, M. J. Maguire, K. Marjani and R. L. Richards, *J. Chem. Soc., Dalton Trans.*, 1997, 4747.
10 J. V. Barkely, B. T. Heaton, C. Jacob, R. Mageswaran and J. T. Sampanthar, *J. Chem. Soc., Dalton Trans.*, 1998, 697.
11 T. Furuhashi, M. Kawano, Y. Koide, R. Somazawa and K. Matsumoto, *Inorg. Chem.*, 1999, **38**, 109.
12 R. R. Schrock, T. E. Glassman, M. G. Vale and M. Kol, *J. Am. Chem. Soc.*, 1993, **115**, 1760.
13 S. M. Malinak, K. D. Demadis and D. Coucouvanis, *J. Am. Chem. Soc.*, 1995, **117**, 3126.
14 T. A. George, D. N. Kurk and J. Redepenning, *Polyhedron*, 1996, **15**, 2377.
15 G. N. Schrauzer, F. R. Robinson, E. L. Moorehead and J. M. Vickery, *J. Am. Chem. Soc.*, 1976, **98**, 2815.
16 Y. Hozumi, Y. Imasaka and T. Tanaka, *Chem. Lett.*, 1983, 897.
17 S. Cai and R. R. Schrock, *Inorg. Chem.*, 1991, **30**, 4106.
18 S. Kuwata, Y. Mizobe and M. Hidai, *Inorg. Chem.*, 1994, **33**, 3619.
19 K. D. Demadis and D. Coucouvanis, *Inorg. Chem.*, 1995, **34**, 3658; K. D. Demadis, S. M. Malinak and D. Coucouvanis, *Inorg. Chem.*, 1996, **35**, 4038; S. M. Malinak, A. M. Simeonov, P. E. Mosier, C. E. Mckenna and D. Coucouvanis, *J. Am. Chem. Soc.*, 1997, **119**, 1662.
20 R. E. Palermo, R. E. Singh, J. K. Bashkin and R. H. Holm, *J. Am. Chem. Soc.*, 1984, **106**, 2600.
21 G. Ramachandraiah, *J. Am. Chem. Soc.*, 1994, **116**, 6733.
22 R. Prakash, B. Tyagi, D. Chatterjee and G. Ramachandraiah, *Polyhedron*, 1997, **12**, 1235.
23 R. Prakash and G. Ramachandraiah, *Stud. Surf. Sci. Catal.*, 1998, **113**, 519; D. Chatterjee, *Coord. Chem. Rev.*, 1998, **168**, 273.
24 R. Prakash and G. Ramachandraiah, *J. Mol. Catal. A, Chem.*, in the press.
25 E. R. Mercer and R. R. Buckley, *Inorg. Chem.*, 1965, **4**, 1962.
26 T. Matsubara and C. Creutz, *Inorg. Chem.*, 1979, **18**, 1956; *J. Am. Chem. Soc.*, 1978, **100**, 6255.
27 A. A. Diamantis and J. V. Dubrawski, *Inorg. Chem.*, 1981, **20**, 1142; M. M. Taqui Khan, A. Kumar and Z. Shirin, *J. Chem. Res.* (*S*), 1986, **5**, 1003.
28 M. M. Taqui Khan, M. A. Moiz and A. Hussain, *J. Coord. Chem.*, 1991, **23**, 245; M. M. Taqui Khan and R. M. Naik, *J. Mol. Catal.*, 1989, **54**, 139.
29 M. M. Taqui Khan, A. Hussain, G. Ramachandraiah and M. A. Moiz, *Inorg. Chem.*, 1986, **25**, 3023; M. M. Taqui Khan and A. Hussain, *Indian J. Chem., Sect. A*, 1979, **19**, 50; *CRC Handbook of Chemistry and Physics*, eds. R. C. Weast and M. J. Astle, CRC Press, Boca Raton, FL, 1979, p. D-168.
30 A. E. Martell and M. Calvin, in *Chemistry of Metal Chelate Compounds*, Prentice-Hall, New York, 1952.
31 L. Meites, in *Polarographic Techniques*, Interscience, New York, 2nd edn., 1957, pp. 95–301.
32 A. J. Bard and L. R. Faulkner, in *Electrochemical Methods Fundamentals and Applications*, Wiley, New York, 1980.
33 V. N. Alexeyev, in *Qualitative Chemical Semimicro Analysis*, ed. P. K. Agasyan, Mir Publishers, Moscow, 1975, p. 475.
34 J. F. Endicott and H. Taube, *Inorg. Chem.*, 1965, **4**, 437; K. Shimzu, T. Matsubara and G. P. Sato, *Bull. Chem. Soc. Jpn.*, 1974, **47**, 1651.
35 P. D. Maria Mattioli and A. A. Luiz Oliveria, *Polyhedron*, 1987, **6**, 603.
36 H. Ogino, T. Watanabe and N. Tanaka, *Inorg. Chem.*, 1975, **14**, 2093; H. Ogino, M. Shimura and N. Tanaka, *Inorg. Chem.*, 1979, **18**, 2497.
37 A. E. Martell and R. M. Smith, in *Critical Stability Constants*, Plenum, New York, 1982, vols. 1–5.

Paper a908338c